PNAS RESEARCH ARTICLE | BIOCHEMISTRY OPEN ACCESS

HER2-driven breast cancer suppression by the JNK signaling pathway

Zeynep Itah[a], Shanzah Chaudhry[a], Sithara Raju Ponny[a], Ozkan Aydemir[a], Alexandra Lee[a], Julie Cavanagh-Kyros[a], Cathy Tournier[b], William J. Muller[c], and Roger J. Davis[a,1]

Contributed by Roger J. Davis; received October 27, 2022; accepted December 16, 2022; reviewed by Anton M. Bennett and Senthil Muthuswamy

The HER2$^+$ subtype of human breast cancer is associated with the malignant transformation of luminal ductal cells of the mammary epithelium. The sequence analysis of tumor DNA identifies loss of function mutations and deletions of the *MAP2K4* and *MAP2K7* genes that encode direct activators of the JUN NH_2-terminal kinase (JNK). We report that in vitro studies of human mammary epithelial cells with CRISPR-induced mutations in the MAPK and MAP2K components of the JNK pathway caused no change in growth in 2D culture, but these mutations promoted epithelial cell proliferation in 3D culture. Analysis of gene expression signatures in 3D culture demonstrated similar changes caused by HER2 activation and JNK pathway loss. The mechanism of signal transduction cross-talk may be mediated, in part, by JNK-suppressed expression of integrin α6β4 that binds HER2 and amplifies HER2 signaling. These data suggest that HER2 activation and JNK pathway loss may synergize to promote breast cancer. To test this hypothesis, we performed in vivo studies using a mouse model of HER2$^+$ breast cancer with *Cre/loxP*-mediated ablation of genes encoding JNK (*Mapk8* and *Mapk9*) and the MAP2K (*Map2k4* and *Map2k7*) that activate JNK in mammary epithelial cells. Kaplan–Meier analysis of tumor development demonstrated that JNK pathway deficiency promotes HER2$^+$-driven breast cancer. Collectively, these data identify JNK pathway genes as potential suppressors for HER2$^+$ breast cancer.

HER2$^+$ breast cancer | JNK | integrin α6β4 | MAP2K4 | MAP2K7

Significance

The cJun NH_2-terminal kinase (JNK) signaling pathway has been implicated in the etiology of breast cancer because mutations in the JNK pathway have been identified in tumors. To test the role of the JNK pathway, we studied an in vitro CRISPR-based model of HER2$^+$ cancer using human mammary epithelial cells and an in vivo mouse genetic model of HER2$^+$ breast cancer. The data obtained demonstrated that JNK deficiency and HER2 signaling caused similar changes in gene expression in 3D cultures of human mammary epithelial cells in vitro. Moreover, JNK deficiency caused accelerated development of mouse breast cancer in vivo. These observations establish a tumor suppression function for the JNK signaling pathway in HER2$^+$ breast cancer.

Human epidermal growth factor receptor 2 (HER2/ErbB2) is overexpressed in approximately 25% of human breast cancers (1). This HER2$^+$ tumor subtype is associated with a gene expression signature that includes inflammation (2). Indeed, the increased expression of interleukin (IL) 1 and IL6 promotes HER2$^+$ breast cancer development (3, 4). Moreover, the concentration of these cytokines in the blood correlates with poor prognosis (5). These inflammatory cytokine circuits represent a potential target of therapeutic intervention (3, 4). Transcription factors implicated in driving this cytokine response include STAT3 and NF-κB (6). Signaling pathways that mediate this response are represented by RAS (7), SRC (6), and JUN NH_2-terminal kinase (JNK) (8). The role of JNK is intriguing because JNK is activated in HER2$^+$ tumors (9) and JNK is implicated in the regulation of inflammatory cytokine expression (10). It is therefore likely that JNK may contribute to the regulation of inflammatory cytokine expression by HER2$^+$ tumors (8).

Whether JNK plays a pro-tumorigenic role in breast cancer is unclear. Initial studies using small molecule inhibitors with poor selectivity for JNK (11, 12) suggest that JNK pathway inactivation suppresses HER2$^+$ breast cancer (9). However, this role of JNK is inconsistent with more recent studies of the mutational landscape of breast cancer that have identified frequent mutations in the JNK pathway (13). The JNK pathway in the mammary ductal epithelium is formed by JNK1 and JNK2 (encoded by the *MAPK8* and *MAPK9* genes), the JNK activators MAP2K4 and MAP2K7, and several MAP3K isoforms (10). The mutation of the *MAPK8* and *MAPK9* genes is detected infrequently. This is most likely because the JNK1 and JNK2 protein kinases function in a largely redundant manner (10). Consequently, compound mutation of both the *MAPK8* and *MAPK9* genes is required to suppress JNK signaling (14). However, the *MAP2K4* and *MAP2K7* genes are partially non-redundant because MAP2K4 selectively phosphorylates JNK on Tyr^{182}, while MAP2K7 selectively phosphorylates JNK on Thr^{180} and dual phosphorylation on Thr^{180} plus Tyr^{182} is required for full JNK activation (15). Indeed, mutation of either MAP2K4 or MAP2K7 suppresses JNK signaling (15). Similarly, MAP3K1 exhibits non-redundant functions and mutational inactivation of MAP3K1 can suppress JNK signaling (16). These considerations indicate that the *MAP3K1*, *MAP2K4*, and *MAP2K7* genes represent potential sites of inactivation of the JNK pathway in breast cancer.

Sequencing human tumor DNA has identified mutations in the genes *MAP3K1*, *MAP2K4*, and *MAP2K7* (17–26). The identified genetic changes include gene copy number reductions and loss-of-function mutations in luminal breast cancer and also gene copy number reductions

Author contributions: Z.I. and R.J.D. designed research; Z.I., S.C., A.L., and J.C.-K. performed research; Z.I., C.T., and W.J.M. contributed new reagents/analytic tools; Z.I., S.R.P., O.A., A.L., and R.J.D. analyzed data; and Z.I., C.T., W.J.M., and R.J.D. wrote the paper.

Reviewers: A.M.B., Yale University School of Medicine; and S.M., National Cancer Institute.

The authors declare no competing interest.

[1]To whom correspondence may be addressed. Email: Roger.Davis@umassmed.edu.

This article contains supporting information online at http://www.pnas.org/lookup/suppl/doi:10.1073/pnas.2218373120/-/DCSupplemental.

Published January 19, 2023.

in HER2^{+} breast cancer. JNK pathway inhibition, rather than JNK pathway activation, is therefore associated with human breast cancer. This conclusion is consistent with the finding that several breast cancer "drivers" (e.g., HER2, PTEN, and PI3K) cause AKT activation and inhibitory phosphorylation of MAP2K4 that suppresses JNK signaling (27). Collectively, these data indicate that loss of JNK signaling may occur frequently in breast cancer.

The purpose of this study was to test the role of the JNK signaling pathway in HER2^{+}-promoted breast cancer using a human model in vitro and a mouse model in vivo. We report that HER2 activation cooperates with JNK pathway suppression to promote breast cancer development. This analysis provides a functional test of the hypothesis that genes that encode JNK pathway components can act as tumor suppressors.

Results

Establishment of Human Mammary Epithelial Cells with Targeted Ablation of JNK Pathway Genes. Human mammary epithelial MCF-10A.B2 cells (28) with ablation of the *MAPK8* plus *MAPK9* genes were generated using CRISPR/*Cas9* technology by insertion of a *puromycin* cassette in the *MAPK8* gene and by the introduction of an InDel in the *MAPK9* gene at the sites of sgRNA-guided *Cas9*-mediated genomic DNA cleavage (*SI Appendix*, Fig. S1 *A* and *B*). Immunoblot analysis demonstrated that the mutant JNK^{KO} cells did not express JNK1 (MAPK8) or JNK2 (MAPK9) (Fig. 1*A*).

To establish an independent model of JNK pathway deficiency, we ablated the *MAP2K4* and *MAP2K7* genes that encode the direct activators of JNK1 and JNK2 (10) by introduction of CRISPR/*Cas9*-induced InDels in these genes (*SI Appendix*, Fig. S1 *A* and *B*). Immunoblot analysis demonstrated that the mutant MKK4/7^{KO} cells expressed JNK1 and JNK2, but not MKK4 (MAP2K4) or MKK7 (MAP2K7) (Fig. 1*B*).

To confirm that the MKK4/7^{KO} and JNK^{KO} cells exhibit a defect in JNK signaling, we examined JNK pathway activation in response to stress (UV-C radiation). Immunoblot analysis using antibodies to pThr^{180} pTyr^{182} JNK1/2 and pSer^{63} JUN demonstrated that exposure to UV-C radiation caused JNK activation and phosphorylation of the JNK substrate JUN in wild-type cells, but not in MKK4/7^{KO} or JNK^{KO} cells (Fig. 1 *C* and *D*). Control studies demonstrated that activation of other MAPK pathways

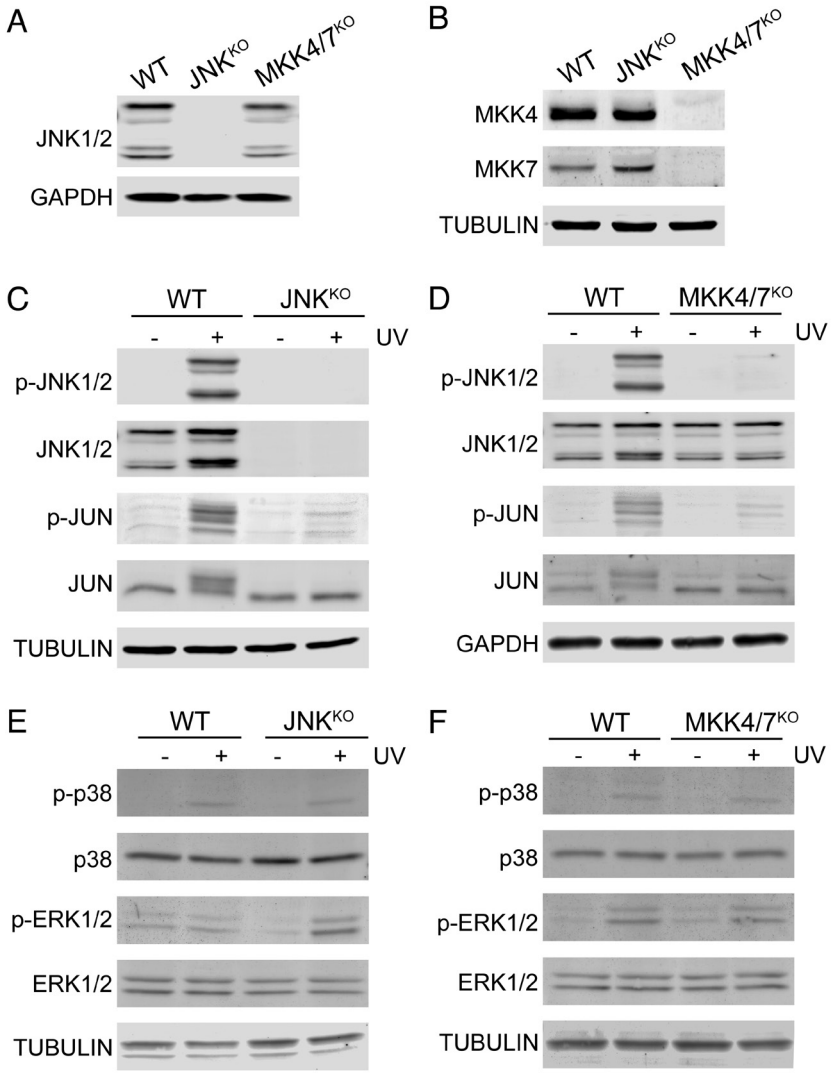

Fig. 1. Disruption of the stress-activated JNK signaling pathway in human mammary epithelial cells. (*A* and *B*) MCF-10A.B2 cells with targeted ablation of the *MAPK8* plus *MAPK9* genes (JNK^{KO} cells) or *MAP2K4* plus *MAP2K7* genes (MKK4/7^{KO} cells) were examined by immunoblot analysis by probing with antibodies to JNK, MKK4, MKK7, and α-Tubulin or GAPDH. (*C*–*F*) Wild-type, JNK^{KO}, and MKK4/7^{KO} cells were treated without (−) or with (+) 60 J/m^2 UV-C. Cell lysates (40 μg) harvested at 15 min post-irradiation were examined by immunoblot analysis by probing with antibodies to p-JUN, JUN, p-JNK1/2, JNK1/2, p-p38, p38, p-ERK1/2, ERK1/2, and α-Tubulin or GAPDH.

(ERK and p38) was similar in wild-type, MKK4/7^{KO}, and JNK^{KO} cells (Fig. 1 *E* and *F*).

Since CRISPR/*Cas9* technology can cause unexpected genomic changes, we performed whole genome sequencing (WGS) on the wild-type (WT), MKK4/7^{KO}, and JNK^{KO} human mammary epithelial MCF-10A.B2 cells. This analysis validated the presence of the anticipated mutations in the *MAP2K4*, *MAP2K7*, *MAPK8*, and *MAPK9* genes (*SI Appendix*, Fig. S1). Potential off-target effects of CRISPR/*Cas9* are anticipated to introduce InDel mutations into the genome. No homozygous off-target InDels were detected. However, one heterozygous InDel was detected in the *POLR1B* gene of MKK4/7^{KO} cells and heterozygous InDels were detected in the *ASB15* and *PREX1* genes of JNK^{KO} cells (*SI Appendix*, Fig. S1 *C* and *D*). The phenotypic consequences of these off-target InDels are likely limited by their heterozygous nature. Moreover, the detected heterozygous InDels are different in the two models of JNK pathway deficiency that we established. These data demonstrate that MKK4/7^{KO} and JNK^{KO} cells provide independent models for studies of JNK pathway deficiency in human mammary epithelial cells.

Mammary Epithelial Cells in Monolayer Culture and JNK Pathway Deficiency. We initially performed studies using human mammary epithelial MCF-10A.B2 cells (28) under standard tissue culture conditions (2D culture). Activated HER2 signaling was modeled in these cells using the B/B homodimerizer drug AP20187 that induces activation of a HA-tagged chimeric rat Neu/ErbB2-FKBP fusion protein that was expressed by an integrated retroviral provirus (28). Whole-genome sequence (WGS) analysis identified the provirus insertion site on Chromosome 5 (hg 38; + strand; 59,106,900 to 59,106,903). Immunoblot analysis demonstrated that B/B-stimulated HER2 signaling caused similar activation of the ERK and AKT pathways in WT, MKK4/7^{KO}, and JNK^{KO} cells (Fig. 2 *A* and *B*).

To mimic later invasive stages of cancer using the MCF-10A.B2 experimental model, we treated cells with TGFβ1 to examine the effect of JNK pathway deficiency on epithelial-mesenchymal transition (EMT). Immunoblot analysis demonstrated that TGFβ1 and B/B caused a similar increase in N-Cadherin expression in WT, MKK4/7^{KO}, and JNK^{KO} cells while treatment with B/B plus TGFβ1 enhanced this increase. In contrast, no change in E-cadherin expression was detected by immunoblot analysis within 24 h of treatment (Fig. 2*C*). Gene expression analysis demonstrated that *CDH1* (encodes E-Cadherin), *CDH2* (encodes N-Cadherin), and *VIM* (encodes vimentin) mRNA were similarly regulated in wild-type, MKK4/7^{KO}, and JNK^{KO} cells in response to TGFβ1 (Fig. 2*D*). These hallmarks of TGFβ1-stimulated EMT were therefore unaffected by JNK pathway deficiency in 2D culture.

To test whether the JNK pathway influenced proliferation, we examined B/B homodimerizer-induced activation of HER2 signaling in 2D culture. A similar increase in the proliferation of WT, MKK4/7^{KO}, and JNK^{KO} cells was detected (*SI Appendix*, Fig. S2*A*). Indeed, we found that treatment with JNK-IN-8, a specific JNK inhibitor (29), caused no change in the rate of proliferation of WT or JNK^{KO} mammary epithelial cells (*SI Appendix*, Fig. S2*B*). These data demonstrate that the JNK pathway does not regulate human mammary epithelial cell proliferation in 2D culture. This observation markedly differs from murine fibroblasts, which undergo *Trp53*-dependent senescence following JNK pathway inhibition (30).

Previous studies of murine fibroblasts demonstrate that JNK deficiency in monolayer culture accelerates scratch wound closure (31). In contrast, scratch wound closure by WT, MKK4/7^{KO}, and JNK^{KO} human mammary epithelial cells was similar under control, B/B-stimulated, TGFβ1-stimulated, and B/B plus TGFβ1-stimulated conditions (*SI Appendix*, Fig. S2*C*). These data indicate that JNK pathway inhibition causes only small changes in HER2-stimulated wound closure by human mammary epithelial cells (*SI Appendix*, Fig. S2*C*). Collectively, these studies demonstrate that only minor phenotypes were detected in JNK pathway-deficient human mammary epithelial cells in 2D culture in vitro.

JNK Pathway Deficiency Promotes Mammary Epithelial Cell Proliferation in 3D Culture. WT MCF-10A.B2 human mammary epithelial cells form single acini with cleared lumens in growth factor reduced (GFR) Matrigel®. In contrast, B/B-promoted HER2 signaling caused the formation of multi-acinar structures with filled lumens (28). The formation of these multi-acini structures was suppressed by TGFβ1 and largely replaced with smaller acini showing invasive phenotypes in GFR Matrigel® (Fig. 3*A*). Similar multi-acinar structures were detected in WT, MKK4/7^{KO}, and JNK^{KO} cells with B/B homodimerizer-induced HER2 activation (Fig. 3*A*). However, JNK pathway deficiency caused a major difference in acinar development under control conditions without B/B homodimerizer or TGFβ1 (Fig. 3*A*). The mean sizes of both total acini and multi-acini were significantly larger in the cultures of MKK4/7^{KO} and JNK^{KO} cells compared with WT cells (Fig. 3*B*), although no significant difference in acini number was detected (Fig. 3*C*). To confirm this observation, we tested the effect of JNK inhibition using the small molecule JNK-IN-8 (29) on the growth of WT MCF-10A.B2 cells in GFR Matrigel®. We found that JNK pathway inhibition increased the formation of multi-acini structures (*SI Appendix*, Fig. S2*D*).

The effect of JNK pathway deficiency on acinar size may reflect an increase in MCF-10A.B2 cell proliferation in 3D culture. No incorporation of EdU by WT acini was detected, but EdU incorporation by JNK^{KO} acini cells was observed (Fig. 3*D*). Quantitation by flow cytometry demonstrated increased EdU incorporation by JNK^{KO} and MKK4/7^{KO} cells compared with WT cells (Fig. 3*E*). Fluorescence microscopy demonstrated that the EdU-positive cells correspond to luminal acinar cells (Fig. 3*D*). These luminal acinar cells were detected in acini formed by MKK4/7^{KO} and JNK^{KO} cells under control conditions, but luminal cells were only detected in WT acini following HER2 pathway activation with B/B homodimerizer (Fig. 3*F*). Collectively, these data indicate that JNK pathway inhibition promotes the proliferation of luminal acinar cells.

JNK Pathway Deficiency Phenocopies the Effects of Oncogenic HER2 Signaling on the Human Mammary Epithelial Cell Transcriptome. We examined gene expression in WT and JNK^{KO} MCF-10A.B2 human mammary epithelial cells grown in 3D culture by RNA-seq analysis. The principal component analysis demonstrated the separation of WT and JNK^{KO} gene expression signatures under different treatment conditions, but co-clustering of the control JNK^{KO} gene signature with the B/B-treated WT gene signature (Fig. 4*A*). Indeed, heatmap analysis of the data confirmed differences between control WT vs. control JNK^{KO} and similarities between B/B-treated WT vs. control JNK^{KO} (Fig. 4*B*). Scatterplot analysis of significantly differentially expressed (DE) mRNA identified 408 genes that were upregulated and 248 genes that were downregulated in control JNK^{KO} vs. control WT (Fig. 4*C*). In contrast, 109 genes were upregulated and 72 genes were downregulated in control JNK^{KO} vs. B/B-treated WT (Fig. 4*D*). This analysis indicated that the effects of JNK pathway blockade and HER2 activation on gene expression are similar. To test this prediction, we performed Venn diagram analysis of DE genes caused by JNK

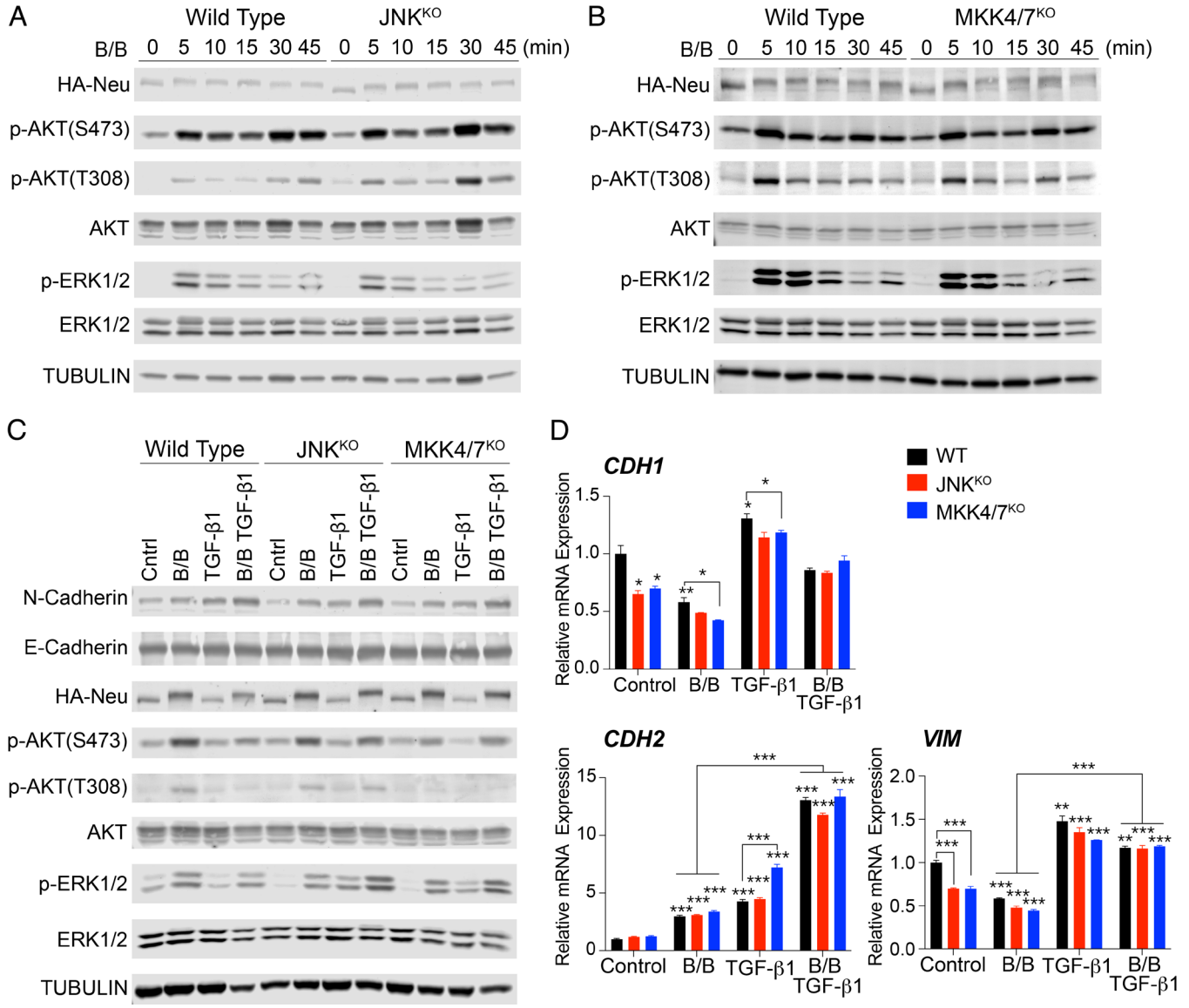

Fig. 2. The JNK pathway is not essential for the HER2 signaling response of human mammary epithelial cells. (*A* and *B*) WT, JNK^{KO}, and MKK4/7^{KO} MCF-10A.B2 cells cultured in starvation medium (24 h) were treated without or with 1 μM B/B homodimerizer to activate HER2 signaling for defined times (0 to 45 min). Cell lysates (40μg) were examined by immunoblot analysis using antibodies to HA, pSer^{473}-AKT, pThr^{308}-AKT, AKT, p-ERK1/2, ERK1/2, and α-Tubulin. (*C* and *D*) WT, JNK^{KO}, and MKK4/7^{KO} MCF-10A.B2 cells cultured in starvation medium (24 h) were treated without (solvent) or with 1 μM B/B homodimerizer and/or 20 ng/mL TGF-b1 (24 h) in serum-depleted medium. Cell lysates were examined by immunoblot analysis by probing with antibodies to N-Cadherin, E-Cadherin, HA, pThr^{308}-AKT and pSer^{473}-AKT, AKT, p-ERK1/2, ERK1/2, and α-Tubulin. The expression of mRNA was quantitated by Taqman® analysis. The expression of *CDH1*, *CDH2*, and *VIM* mRNA (normalized to *GAPDH* mRNA) is presented as the mean ± SEM, n = 3, $*P < 0.05$, $**P < 0.01$, $***P < 0.001$, unpaired *t* test) and are representative of three independent experiments.

deficiency under control conditions and DE genes caused by B/B treatment of WT cells (Fig. 4*E*). This analysis identified 440 genes that were similarly regulated by B/B treatment of WT cells and JNK pathway inhibition (Fig. 4*E*). Gene set enrichment analysis (GSEA) of DE genes caused by JNK deficiency under control conditions reported hallmarks of apical junctions, KRAS signaling, and breast cancer pathways (Fig. 4*F*).

Pathway analysis of the RNA-seq data indicated that integrin signaling is increased in JNK-deficient mammary epithelial cells (*SI Appendix*, Fig. S3*A*) and is associated with increased integrin expression, including the laminin receptor α6β4 (*SI Appendix*, Fig. S3*B*). This observation is interesting because α6β4 binds HER2 and promotes HER2 signaling and breast tumor development (32). Integrin α6β4 may therefore mediate, in part, signal transduction cross-talk between JNK and HER2 in breast tumor development.

To further test the role of JNK signaling, we examined miRNA expression signatures. Principal component analysis of small RNA-seq data demonstrated the separation of control WT and control JNK^{KO} miRNA expression signatures and co-clustering of B/B treated-WT and control JNK^{KO} miRNA expression signatures (Fig. 5*A*). DE miRNA profiles of these conditions were examined by heatmap analysis (Fig. 5*B*). Scatterplot analysis identified 108 upregulated and 91 downregulated DE miRNAs in control JNK^{KO} compared with control WT (Fig. 5*C*). However, only 18 upregulated and 11 downregulated DE miRNAs were detected in the comparison of control JNK^{KO} vs. B/B-treated WT (Fig. 5*C*). We used computational tools to identify predicted DE mRNA targets of these DE miRNAs in the control JNK^{KO} vs. control WT comparison. The expression levels of these mRNA targets were examined using RNA-seq data. A total of 419 predicted miRNA target

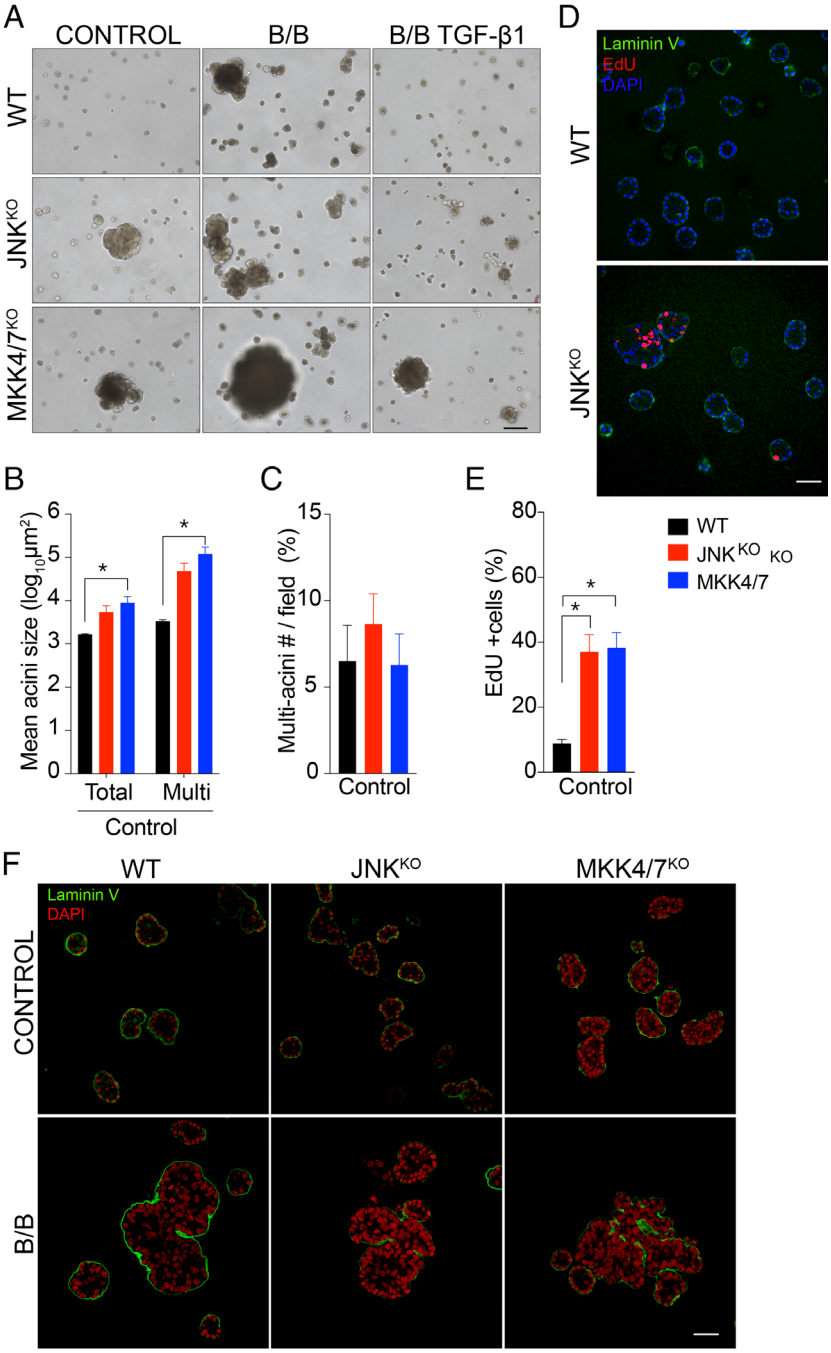

Fig. 3. The JNK pathway suppresses the proliferation of luminal epithelial mammary cells and the formation of multi-acinar structures. (*A*) WT, JNK^{KO}, and MKK4/7^{KO} MCF-10A.B2 cells were plated on GFR Matrigel® in Assay Medium supplemented with EGF (7 d). The EGF was replaced with 1μM B/B homodimerizer (or solvent) and/or 20 ng/mL TGF-β1 and the cells were cultured for 14 more days. Images that are representative of three independent experiments obtained using a Zeiss Axiovert 200M microscope (×10 objective) are presented (Scale bar, 200 μm.). (*B* and *C*) Acini and multi-acini images were quantitated using ZEN AxioVision 4.8 software (160 acini per condition) with the investigator blinded to both genotype and treatment condition. The data presented are representative of three independent experiments (mean ± SEM; n = 160; *P < 0.05, ***P < 0.001). (*D* and *E*) Acinar cell proliferation under Control conditions on day 21 was examined by measurement of EdU incorporation (24 h). EdU incorporation was examined by (*D*) fluorescence microscopy of cells stained using an antibody to the basement membrane marker Laminin V (green) and nuclear staining of EdU (red) and DAPI (blue) (Scale bar, 50 μm) and (*E*) flow cytometry (mean ± SEM, *P < 0.05, n = 2). (*F*) Acinar structures were examined on day 21 by immunofluorescence analysis using Laminin V (green) and DAPI (red) staining (Scale bar, 50 μm.).

mRNAs were identified (Fig. 5*D*). GSEA of these genes reported hallmarks of KRAS signaling, mTORC1 signaling, TGFβ signaling, and apoptosis (Fig. 5*E*).

The identification of a TGFβ pathway gene signature in the JNK^{KO} cells by GSEA was unexpected (Fig. 5*E*) because increased TGFβ responsiveness was only a modest phenotype of cells grown in 2D culture (Fig. 2*D*). However, heatmap analysis of DE mRNA (Fig. 4*B*), DE miRNA (Fig. 5*B*), and predicted DE mRNA targets of DE miRNA (Fig. 5*D*) demonstrated increased TGFβ responsiveness of JNK^{KO} cells compared with WT cells in 3D culture. It is possible that reduced JNK-mediated inhibitory phosphorylation of the transcription factor SMAD2 (33) contributes to this increased responsiveness of JNK^{KO} cells to TGFβ.

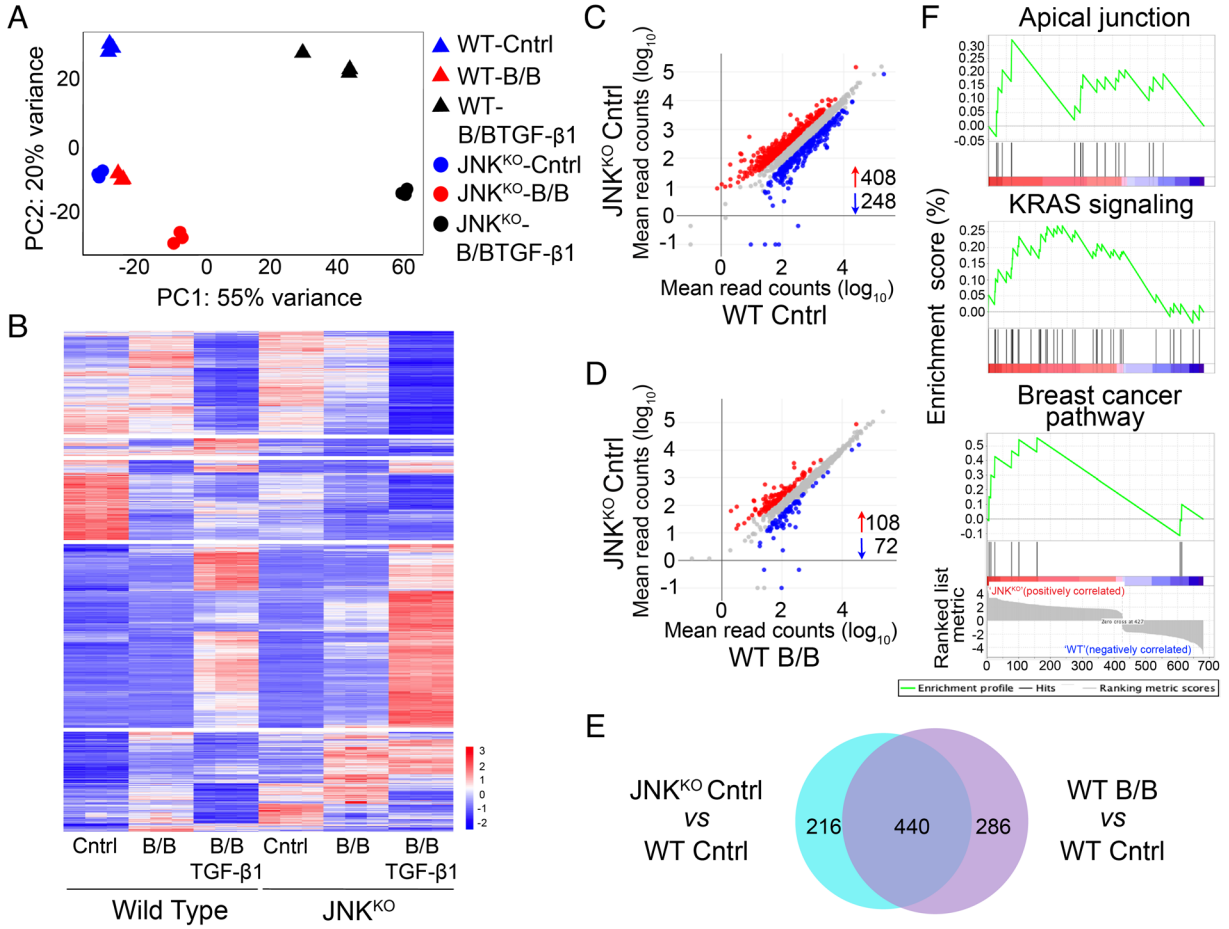

Fig. 4. JNK deficiency promotes an activated HER2-like mRNA transcriptome. (*A* and *B*) WT and JNK^{KO} MCF-10A.B2 mammary epithelial cells in 3D culture (21 d) were examined by RNA-seq analysis to detected differentially expressed (DE) mRNAs (|log2FC|>1, p_{adj} < 0.01, n = 3). The effects of solvent (Cntrl, control), 1 μM B/B homodimerizer without or with 20 ng/mL TGF-β1 were examined. Principal component analysis (*A*) and heatmap analysis of the DE genes (κ-means = 5) (*B*) are presented. (*C*–*E*) Scatter plot representation of mean read counts of DE genes of JNK^{KO} control (Cntrl) vs. WT Cntrl (*C*) and JNK^{KO} Cntrl vs. WT B/B (*D*). Upregulated genes (red), downregulated genes (blue), and nonsignificant changes (gray) are indicated. The DE gene data are also presented as a Venn Diagram (*E*). (*F*) GSEA of JNK^{KO} Cntrl vs. WT Cntrl DE genes performed using hallmark gene sets is presented (gene set size filters; min = 3, max = 1,000, *P* value < 0.001).

Collectively, these data demonstrate that JNK signaling deficiency partially mimics the effects of activated HER2 signaling on gene expression in 3D cultured mammary epithelial cells. Moreover, JNK pathway deficiency increases the gene expression response of these cells to TGFβ.

HER2-Induced Mammary Carcinoma Is Promoted by JNK Pathway Deficiency In Vivo. We have previously reported that ablation of the *Mapk8* plus *Mapk9* genes in luminal murine mammary epithelial cells causes ductal occlusion with infiltrating epithelial cells (34). This in vivo phenotype resembles the in vitro phenotype of human mammary epithelial cells with JNK pathway inhibition that exhibit increased multi-acinar size and luminal occlusion (Fig. 3). Similarly, activated HER2 promotes luminal occlusion and increased acinar size in vitro (Fig. 3). Indeed, similar effects of JNK pathway inhibition and HER2 activation on gene expression were detected (Figs. 4 and 5).

We tested whether JNK pathway inhibition altered HER2-promoted breast cancer using a mouse model. *MMTV-NIC*$^{+}$ mice express an activated *Neu* allele with an IRES-*Cre* cassette inserted in the 3′ UTR (35). These mice develop luminal breast cancer with a latency of approximately 150 d (Fig. 6*A*). We established *MMTV-NIC*$^{+}$ mice on a WT background and a JNK-deficient (JNK^{KO}) background (*MMTV-NIC*$^{+}$ *Mapk8*$^{loxP/loxP}$ *Mapk9*$^{loxP/loxP}$). We found that the deficiency of JNK1 plus JNK2 in mammary epithelial cells significantly ($P < 0.0001$) accelerated the development of breast cancer (Fig. 6*A*). Similarly, *MMTV-NIC*$^{+}$ *Map2k4*$^{loxP/loxP}$ (MKK4^{KO}) mice ($P < 0.0001$) and *MMTV-NIC*$^{+}$ *Map2k7*$^{loxP/loxP}$ (MKK7^{KO}) mice ($P < 0.0002$) also exhibited significantly accelerated breast tumor development. The histological examination of hematoxylin and eosin-stained tissue sections by a board-certified pathologist demonstrated the presence of similar mammary intraepithelial neoplasia (MIN) lesions and mammary carcinomas in control WT mice and JNK pathway-deficient mice (JNK^{KO}, MKK4^{KO}, and MKK7^{KO}) with 1-cm^{3} tumors at necropsy (Fig. 6*B*). The analysis of tumor mRNA demonstrated similar gene signatures of hypoxia and angiogenesis (*Vegfa*, *Slc2a2,* and *Pecam1*) and inflammation (*Adgre1*, *Il1*, and *Il6*) in WT and JNK^{KO} tumors (*SI Appendix*, Fig. S4*A*).

The accelerated development of tumors in mice with JNK pathway-deficient mammary epithelial cells (Fig. 6*A*) may result from earlier tumor initiation. We therefore examined young WT and JNK^{KO} MMTV-NIC^{+} mice to investigate an early stage of carcinogenesis. We found MIN lesions in all mice examined. Mammary carcinoma was detected in 4/5 JNK^{KO} mice and 2/6 WT mice at age 12 wk (*SI Appendix*, Fig. S4*B*). This observation is consistent with more rapid tumor development in JNK pathway-deficient mice (Fig. 6*A*).

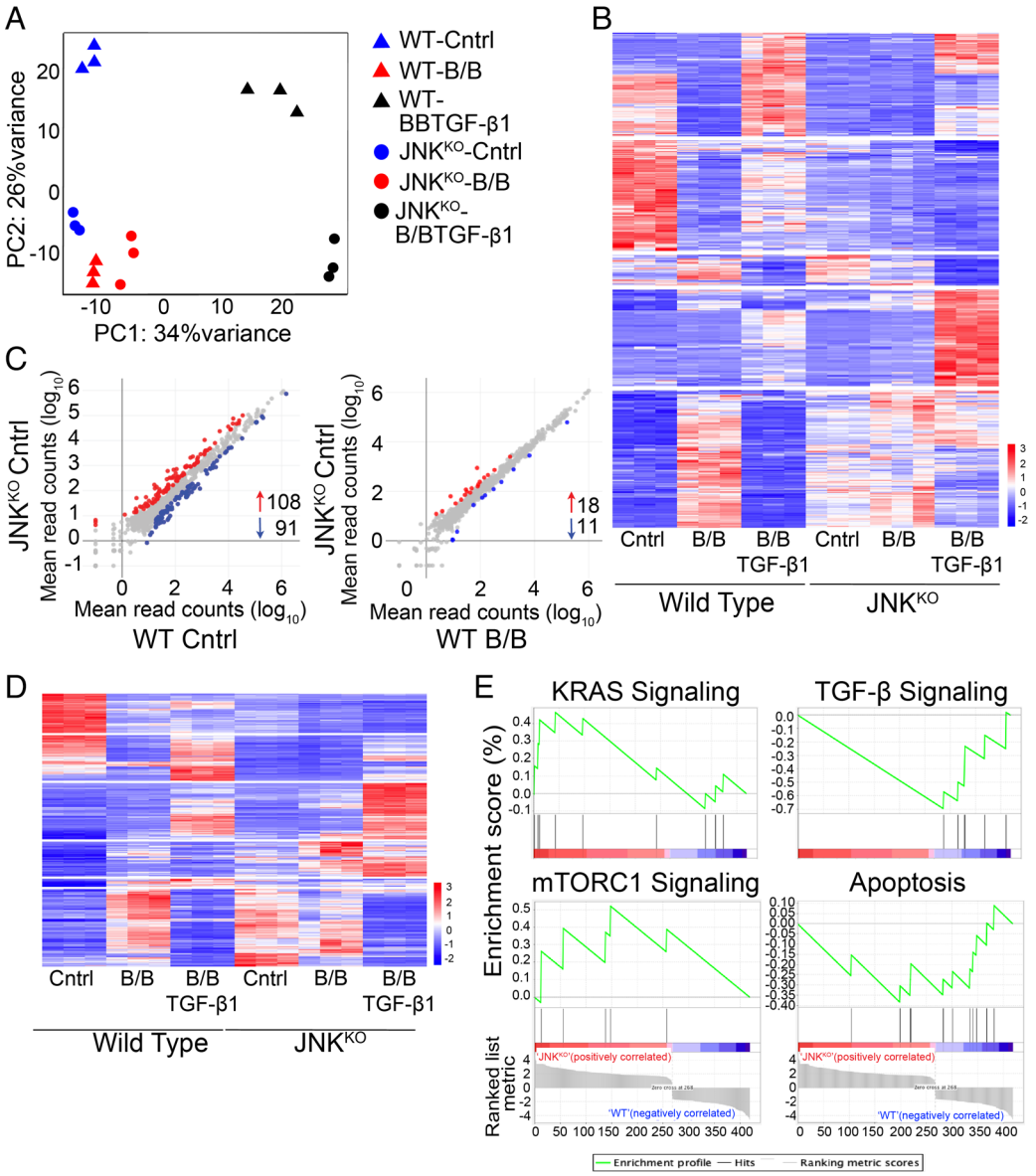

Fig. 5. JNK deficiency promotes an activated HER2-like microRNA transcriptome. (*A* and *B*) WT and JNK^{KO} MCF-10A.B2 mammary epithelial cells in 3D culture (21 d) were examined by small RNA-seq analysis to detected differentially expressed (DE) miRNAs (|log2FC| > 1, p_{adj} < 0.01, n = 3). The effects of solvent (Cntrl, control), 1 μM B/B homodimerizer without or with 20 ng/mL TGFβ1 were examined. Principal component analysis (*A*) and heatmap analysis of the DE genes (κ-means = 5) (*B*) are presented. (*C*) Scatter plot representation of mean read counts of DE miRNA of JNK^{KO} Cntrl vs. WT Cntrl and JNK^{KO} Cntrl vs. WT B/B. Upregulated miRNA (red), downregulated miRNA (blue), and nonsignificant changes (gray) are indicated. (*D*) Predicted mRNA targets of JNK^{KO} Cntrl vs. WT Cntrl DE miRNAs are represented with a heatmap analysis (κ-means = 6). (*E*) Predicted mRNA targets of JNK^{KO} Cntrl vs. WT Cntrl DE miRNA were examined by GSEA using hallmark gene sets (gene set size filters; min = 3, max = 1,000, *P* value < 0.001).

Primary Breast Tumor Cells Exhibit JNK-Dependent Changes in Gene Expression. We established primary mammary tumor cell lines from the murine carcinomas that we obtained. Genotype analysis demonstrated that the tumor cells were WT, JNK^{KO} (*Mapk8*$^{\Delta/\Delta}$ *Mapk9*$^{\Delta/\Delta}$), MKK4^{KO} (*Map2k4*$^{\Delta/\Delta}$), or MKK7^{KO} (*Map2k7*$^{\Delta/\Delta}$) (*SI Appendix*, Fig. S4*C*). Immunoblot analysis demonstrated that the WT tumor cells expressed JNK1 and JNK2 that were phosphorylated and activated by exposure of the cells to stress (UV-C), but no JNK was detected in JNK^{KO} tumor cells (Fig. 6*C*). In contrast, MKK4^{KO} and MKK7^{KO} tumor cells demonstrated reduced JNK activation (Fig. 6*D*), consistent with the known functions of MAP2K4 and MAP2K7 as partially non-redundant activators of JNK (15). No major changes in the activation of other MAPK (ERK and p38 MAPK) were detected (Fig. 6 *C* and *D*). The measurement of tumor cell proliferation demonstrated that JNK^{KO} cells grew at a slower rate than WT tumor cells and that the MKK4^{KO} and MKK7^{KO} tumor cells exhibited an intermediate proliferation phenotype (Fig. 6*E*).

We examined gene expression in six independent WT and seven independent JNK^{KO} primary tumor cell lines by RNA-seq analysis. While some variability between cell lines was detected (*SI Appendix*, Fig. S5*A*), we identified 508 DE genes that were upregulated and 558 DE genes that were downregulated in JNK^{KO} tumor cells compared with WT tumor cells (Fig. 7*A*). GSEA of these genes reported hallmarks of Trp53 signaling, KRas signaling, TNFα signaling via NF-κB, and EMT (Fig. 7*B*). Interestingly, analysis of *keratin* gene expression demonstrated that the WT tumor cells exhibited a luminal phenotype characterized by *Krt8* gene expression, but the JNK^{KO} tumor cells expressed both basal (*Krt5*) and luminal (*Krt8*) markers (*SI Appendix*, Fig. S5 *B* and *C*). JNK pathway inhibition therefore appears to dysregulate tumor cell gene expression and this may contribute to accelerated tumor

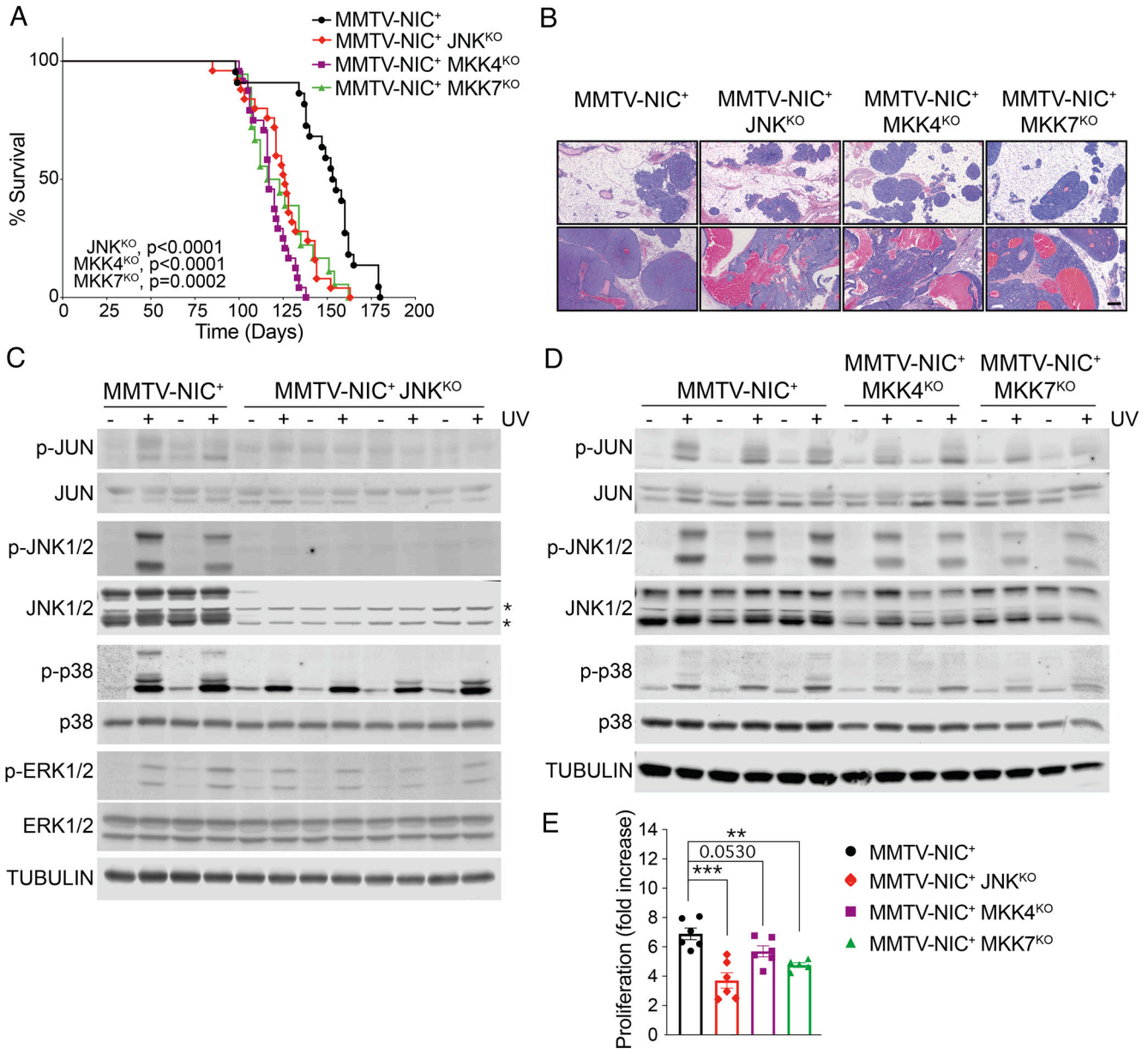

Fig. 6. JNK pathway blockade accelerates tumor formation. (*A*) Kaplan–Meier analysis of mouse survival. All mice with 1-cm^3 tumors were euthanized. Female MMTV-NIC$^+$ mice: WT (n = 22 mice); JNK^{KO} (n = 25 mice); MKK4^{KO} (n = 24 mice); and MKK7^{KO} (n = 18 mice). (*B*) Sections of mammary glands obtained during necropsy were stained with H&E. Representative images of fields with MIN lesions (*Upper*) and mammary gland carcinomas with vascular channels (*Lower*) are presented (Zeiss AxioVert microscope). (Scale bar, 200 μm.) (*C* and *D*) Independent primary MMTV-NIC$^+$ breast cancer cell lines were examined: WT (n = 5); JNK^{KO} (n = 4); MKK4^{KO} (n = 2), and MKK7^{KO} (n = 2). The cells were serum-starved (24 h) and either exposed without or with 60 J/m^2 UV-C. Cell lysates were harvested at 15 min post-irradiation and examined by immunoblot analysis using antibodies to JUN, p-JUN, JNK, p-JNK1/2; p38; p-p38; ERK, p-ERK; and α-Tubulin. *, background band. (*E*) The proliferation rates (0 to 48 h) of MMTV-NIC$^+$ primary murine tumor cell lines [WT (n = 6), JNK^{KO} (n = 6), MKK4^{KO} (n = 6), and MKK7^{KO} (n = 5)] were examined by IncuCyte Zoom analysis (mean ± SEM, $^{**}P < 0.01$, $^{***}P < 0.001$).

development (Fig. 6*A*). This is consistent with the finding that non-luminal human HER2$^+$ breast cancer exhibits poor prognosis compared with luminal HER2$^+$ breast cancer (36–38).

Primary Breast Tumor Cells Exhibit JNK-Dependent Genomic Structural Variations. We performed WGS analysis of WT (n = 6) and JNK^{KO} (n = 7) HER2$^+$ primary tumor cell lines. We initially compared WT and JNK^{KO} genomes for short sequence variant differences (<10 bases), including MNP (multiple nucleotide polymorphism), SNP (single nucleotide polymorphism), deletions, and insertions. No significant differences between WT and JNK^{KO} tumor cells were detected (Fig. 7*C*). We also examined genomic structural variations, including deletions, duplications, insertions, inversions, and translocations (Fig. 7*D*). This analysis demonstrated that the JNK^{KO} tumor cells exhibited an increased number of deletions, insertions, and inversions compared with WT tumor cells (Fig. 7*D*). Indeed, predictions for high-impact inversions that involve exon sequences were significantly increased in JNK^{KO} tumors compared with WT tumors (*SI Appendix*, Fig. S6). Collectively, these data indicate that JNK^{KO} tumors have a higher mutational burden than WT tumors. It is possible that this increased mutational burden contributes to the accelerated tumor development in JNK^{KO} mice compared to WT mice (Fig. 6*A*).

To further examine mutations in WT and JNK^{KO} tumor cells, we performed copy number variation (CNV) analysis to identify deletions and amplifications of genomic DNA (*SI Appendix*, Figs S7 and S8). Principle component analysis demonstrated some variability between independently isolated tumor cell lines of the

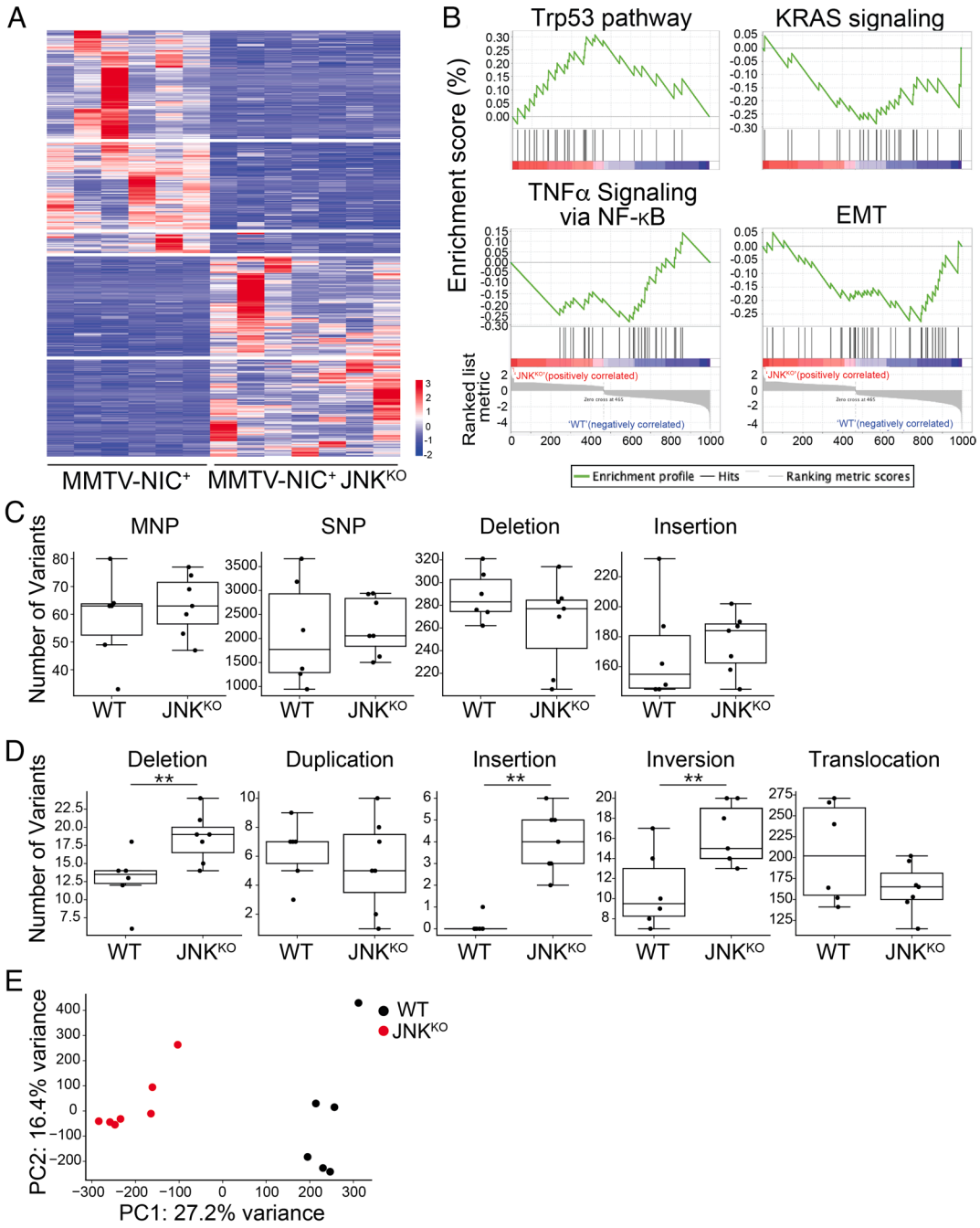

Fig. 7. Primary breast tumor cells exhibit JNK-dependent changes in gene expression and genomic structural variations. (*A*) RNA-seq analysis of MMTV-NIC$^+$ WT (n = 6) and MMTV-NIC$^+$ JNK^{KO} (n = 7) primary mouse breast cancer cell lines. The significant DE genes are presented as a heatmap (κ-means = 5, |log2FC| > 1, p_{adj} < 0.05). (*B*) The significant DE genes of WT vs. JNK^{KO} tumor cells were examined by GSEA using hallmarks of cancer datasets (gene set size filters; min = 3, max = 1,000, *P* value < 0.001). (*C*) WGS analysis of WT (n = 6) vs. JNK^{KO} (n = 7) primary tumor cell lines was examined to detect short sequence variant differences, including MNP (multiple nucleotide polymorphism), SNP (single nucleotide polymorphism), deletions and insertions (box and whiskers plots; Mann–Whitney test, *P* > 0.05). (*D*) WGS data were used to examine genomic structural variants (box and whiskers plots; Mann–Whitney test, **P < 0.01). (*E*) Principal component analysis of CNVs detected in WT (n = 6) and JNK^{KO} (n = 7) primary tumor cell lines.

same genotype (Fig. 7*E*). Nevertheless, the CNV data clustered separately for the WT and JNK^{KO} genotypes, indicating that JNK pathway inhibition influenced the CNV repertoire (Fig. 7*E*). This observation is consistent with the presence of different CNVs in WT and JNK^{KO} tumor cells (*SI Appendix*, Figs. S7 and S8). Examples include differential deletions in chromosomes 1, 3, 4, 14, 19, and X in WT compared with JNK^{KO} tumor cells (*SI Appendix*, Fig. S7) and differential amplifications in chromosomes 1, 11, 14, 16, and 19 in JNK^{KO} compared with WT tumor cells (*SI Appendix*, Fig. S8). Among these, chromosomes 14 and 19 are especially intriguing because both chromosomes exhibited significantly increased amplifications and decreased deletions in JNK^{KO} compared to WT tumor cells. The recurrent JNK-dependent chromosomal alterations may contribute to the more rapid development of HER2$^+$ breast cancer caused by JNK pathway mutations. However, it is also possible that the chromosomal alterations are a consequence (rather than a cause) of the rapid tumor development caused by JNK pathway deficiency.

Discussion

It is established that the JNK pathway is essential for the proliferation of primary fibroblasts because JNK deficiency causes an early senescence phenotype that results from increased *Trp53* gene expression (14, 30). Interestingly, this senescence phenotype was not detected in human mammary epithelial MCF-10A.B2 cells (*SI Appendix*, Fig. S2). Thus, epithelial cell proliferation was not suppressed in *MAPK8*$^{-/-}$ *MAPK9*$^{-/-}$ (JNK^{KO}) cells or *MAP2K4*$^{-/-}$*MAP2K7*$^{-/-}$ (MKK4/7^{KO}) cells (*SI Appendix*, Fig. S2*A*). Moreover, treatment of mammary epithelial cells with the potent and selective inhibitor JNK-IN-8 (29) caused no change in proliferation (*SI Appendix*, Fig. S2*B*). These data indicate that the role of JNK in epithelial cell proliferation is markedly different than fibroblasts.

While no proliferation phenotype caused by JNK deficiency was detected when human epithelial cells were grown in 2D culture conditions, we found that JNK caused a major change in epithelial cell proliferation under 3D culture conditions. JNK pathway deficient epithelial cells (JNK^{KO} and MKK4/7^{KO}) (Fig. 3) and WT cells treated with JNK-IN-8 (*SI Appendix*, Fig. S2*D*) formed large multi-acinar structures that resembled acini induced by HER2 activation. This finding demonstrated that JNK serves to suppress proliferation in fully formed WT acini and that JNK deficiency promotes continued proliferation of luminal epithelial cells within acini (Fig. 3*D*).

This JNK-dependent proliferation phenotype in 3D culture occurs in the context of a defect in JNK-regulated apoptosis. It is established that pro-apoptotic signaling by JNK is required for anoikis of mammary ductal epithelial cells mediated by JNK-regulated BH3-only members of the BCL2 family (39). JNK deficiency in the mammary epithelium therefore causes ductal occlusion (39, 40). This early ductal carcinoma in situ (DCIS)-like phenotype precedes the development of breast cancer in >18-mo-old mice (34). Collectively, these observations indicate that epithelial cell JNK is important for normal mammary gland physiology. This is illustrated by the requirement of JNK for the dynamic regulation of the mammary epithelium during postpartum cycles of involution and regeneration. This process requires JNK function for efficient completion of involution (41) and for the proper regeneration of the ductal epithelium (34).

Tumor Suppressor Function of JNK Pathway Genes. Studies of a mouse model of HER2-promoted breast cancer demonstrated that JNK deficiency caused more rapid tumor development (Fig. 6*A*). Similar observations were made in studies of mice with *Map2k4* or *Map2k7* gene ablation in the mammary epithelium (Fig. 6*A*). It is likely that these findings are relevant to disease because deletion and loss-of-function mutations of *MAP2K4* and *MAP2K7* are detected in human cancer. The presence of these mutations, together with our functional studies of the *Map2k4* or *Map2k7* genes in mice, identify these genes as tumor suppressors. The tumor suppression function of both *MAP2K4* and *MAP2K7* is most likely related to their non-redundant functions as activators of JNK because MAP2K4 selectively phosphorylates JNK on Tyr^{182}, while MAP2K7 selectively phosphorylates JNK on Thr^{180} and dual phosphorylation on Thr^{180} plus Tyr^{182} is required for full JNK activation (15). In contrast, the genes that encode JNK in the mammary epithelium (*MAPK8* and *MAPK9*) are infrequently mutated in human breast cancer (13) most likely because compound mutation of *Mapk8* plus *Mapk9* is required to inhibit JNK signaling (14). This requirement for compound mutation of both genes may account for the low frequency of *MAPK8* and *MAPK9* mutation in human breast cancer.

The phenotype caused by MAP2K4 and MAP2K7 deficiency in *KRas*-promoted pancreatic cancer (42) and *Pten* deficiency-driven prostate cancer (43) has been examined. This analysis demonstrated a dramatic enhancement of tumor formation in compound mutant mice with ablation of the *Map2k4* plus *Map2k7* genes (42, 43). In contrast, only moderate phenotypes were detected in mice with ablation of *Map2k4* or *Map2k7* alone (42, 43). This finding contrasts with our observations of HER2^{+} breast cancer where ablation of *Map2k4* or *Map2k7* alone caused a phenotype similar to compound *Mapk8* plus *Mapk9* gene ablation (Fig. 6*A*). These data indicate that HER2^{+} breast cancer may be more susceptible to the tumor suppressive activity of the *Map2k4* and *Map2k7* genes than *Pten* deficiency-driven prostate cancer or *KRas*-promoted pancreatic cancer.

JNK Suppresses HER2-Driven Breast Cancer. The similar effects of activated HER2 signaling and JNK pathway inhibition on the transcriptome of 3D cultured human mammary epithelial cells (Figs. 4 and 5) and on the formation of enlarged multi-acinar structures (Fig. 3) suggest that HER2 signaling may cooperate with loss of JNK function to promote breast cancer. The mechanism of signal transduction cross-talk may be mediated, in part, by JNK-suppressed expression of integrin α6β4 (*SI Appendix*, Fig. S3) that binds HER2 and promotes HER2 signaling and breast tumor development (32). Indeed, mice with *Mapk8* plus *Mapk9* deficiency in the mammary epithelium (JNK^{KO} mice) exhibited rapid development of HER2^{+} breast cancer compared with control mice (Fig. 6*A*). Rapid HER2^{+} breast tumor development was also detected in mice with *Map2k4* or *Map2k7* deficiency in the mammary epithelium (MKK4^{KO} and MKK7^{KO} mice) compared with control mice (Fig. 6*A*). Mechanisms that account for the increase in tumorigenesis may include the effects of JNK pathway deficiency to cause dysregulated proliferation and suppression of anoikis. JNK signaling may also suppress the mutational landscape of newly arising tumors because of JNK-mediated phosphorylation of SIRT6 that promotes DNA double-strand break repair (44) and JNK-mediated phosphorylation of DGCR8 that induces transcription-coupled nucleotide excision repair (45). However, it is unclear whether the increased mutational burden of JNK pathway-deficient tumors (Fig. 7 *C*–*E* and *SI Appendix*, Figs. S6–S8) is the direct consequence of JNK-regulated DNA repair defects.

JNK-Promoted Inflammation and Breast Cancer. Paracrine inflammatory cytokine circuits function to promote the development of HER2^{+} breast cancer (3, 4) and the JNK signaling pathway is implicated in this process (10). We were therefore surprised to find that JNK deficiency in mammary epithelial cells did not suppress hallmarks of tumor inflammation, including macrophage infiltration and the expression of the inflammatory cytokines IL1 and IL6 (*SI Appendix*, Fig. S4 *A* and *B*). This failure to suppress inflammation is consistent with the observation that JNK pathway inhibition in mammary epithelial cells did not prevent HER2^{+} tumor development (Fig. 6*A*). The simplest explanation for these findings is that the primary site of JNK function to promote tumor-associated inflammation is the tumor microenvironment (46). Indeed, JNK in myeloid cells has been demonstrated to contribute to the development of hepatocellular carcinoma (47). Further studies are required to determine whether JNK plays a similar role in the tumor microenvironment of HER2^{+} breast cancer.

Conclusions

We report that JNK pathway deficiency in human mammary epithelial cells causes dysregulated growth selectively in 3D culture in vitro. We find that the effects of JNK pathway deficiency and activated HER2 on the transcriptome are similar. These observations suggest that JNK pathway deficiency may promote tumor

formation. Indeed, JNK pathway deficiency caused rapid development of HER2$^+$ breast cancer in a mouse model. This analysis demonstrates that JNK pathway genes that are mutated in breast cancer can function to suppress tumor development.

Materials and Methods. Reagents, equipment, and software used in this study are described in *SI Appendix*, Table S1.

Human Mammary Epithelial Cells. Human mammary epithelial MCF-10A.B2 cells were provided by Dr. Senthil Muthuswamy (Beth Israel Deaconess Medical Center, Boston, MA). These cells respond to the B/B homodimerizer by activating ErbB2 signaling and provide a model of HER2$^+$-driven breast cancer (28). The B/B homodimerizer AP20187 binds FK506 Binding Protein 12 (FKBP12) and causes activation of FKBP-tagged cell surface receptors by dimerization (48). The MCF-10A.B2 cells were subcloned and subjected to whole-genome sequencing to identify the site of integration of the *Neu/ErbB2* cassette, which was localized to chromosome 5: 59,106,900-59,106,903 (+ strand; hg38). The inserted *Neu/ErbB2* cassette was detected by PCR amplification of genomic DNA with primers 5′-TGAGCTTCCTTTGGAAAGGTGTGA-3′ and 5′-CTGTTTGCATCCGAATCGTGGTC-3′ (810 bp).

The cells were maintained in growth medium that was composed of DMEM/F12 (Thermo Scientific Cat# 11039-047) media containing 5% horse serum and supplemented with 20 ng/mL EGF (PeproTech Cat# AF-100-15), 10 μg/mL insulin (Sigma Cat# I-1882), 1 ng/mL cholera toxin (Sigma Cat# C8052), 100 μg/mL hydrocortisone (Sigma Cat# H-0888), and 50 U/mL penicillin plus 50 μg/mL streptomycin (Thermo Fisher Scientific Cat# 15140122) and passaged every 2 or 3 d.

Studies were performed by allowing the cells to adhere overnight prior to starvation (24 h) in growth media without serum and EGF. The cells were then treated in serum-depleted growth media (1% horse serum without EGF) with either 1 μM B/B homodimerizer (Clontech Cat# 635058) or 20 ng/mL recombinant human TGFβ1 (R&D Systems Cat# 240B010) or B/B plus TGFβ1. The solvent (ethanol) was used for treatments without B/B.

Mutational Analysis of Human Mammary Epithelial Cells Using CRISPR/Cas9. The *MAPK8*$^{-/-}$ *MAPK9*$^{-/-}$ cell line was generated by transient transfection of MCF-10A.B2 cells with plasmids encoding *Cas9* and guide RNA (sgRNA). *MAPK8* and *MAPK9* genes were ablated sequentially. *MAPK8* gene ablation was performed using MCF-10A.B2 cells transfected using 3μl of FUGENE HD (Promega) with 0.5 μg each of the plasmids JNK1 CRISPR/Cas9 KO (Santa Cruz Cat# sc-424053) and JNK1 HDR plasmids (Santa Cruz Cat# sc-424053-HDR). The *MAPK9* gene was ablated by transfection with 1 μg of the plasmid pX330-U6-Chimeric_BB-CBh-hSpCas9 plasmid (RRID: Addgene_42230) that expresses both sgRNA and *SpCas9*. The *MAPK9* sgRNA GAGTTTGGTTCTGAAAAGGA was designed to target *MAPK9 (*Exon3) using the CRISPR design tool (http://tools.genome-engineering.org) (49). The *MAPK8* gene was ablated by HDR-mediated insertion of a *puromycin* cassette at the site of *Cas9*-mediated genomic DNA cleavage. The MCF-10A.B2 cells were cloned by serial dilution in 96-well plates and selected with 1.5 μg/mL puromycin (Thermo Fisher Scientific Cat# A1113803) at 48 h post-transfection (10 d). *MAPK9* gene ablation was characterized by Sanger sequence analysis (Macrogen) of PCR-amplified *MAPK9* genomic DNA fragments using primers 5′-GGATTGCTGAACCCCATCT-3′ and 5′-TCCTTAGCTTATCCTAGGTCTGAACTC-3′ and analyzed using TIDE (50). Clones were screened by immunoblot analysis using an antibody to JNK1/2 (BD Biosciences Cat# 554285, RRID:AB_395344).

To ablate the *MAP2K4 and MAP2K7* genes, we established MCF-10A.B2 cells that express doxycycline-inducible *Cas9*. MCF-10A.B2 cells were transduced with lentivirus prepared by co-transfection of Phoenix-Ampho cells with the plasmid pCW-Cas9 (Addgene Cat# 50661, RRID:Addgene_50661) together with plasmids psPAX2 (Addgene Cat# 12259, RRID: Addgene_12259) and pMD2.G (Addgene Cat# 12260, RRID: Addgene_12260) (51). At 48 h post-infection, the cells were cloned by serial dilution in 96 well plates and selected with 1.5 μg/mL puromycin (10 d). sgRNAs were designed using CRISPR design (http://tools.genome-engineering.org) and CHOPCHOP tools (https://chopchop.cbu.uib.no). The sgRNAs that target *MAP2K4* Exon 3 (GAAATTGGACGAGGAGCTTA) and *MAP2K7* Exon 3 (GCTCCCGCTGGCCAACGATG) were inserted in the plasmid pLX-sgRNAs (Addgene #50662, RRID: Addgene_50662) and pooled lentiviruses were prepared to ablate *MAP2K4* and *MAP2K7* simultaneously. Cells were selected using 4 μg/mL blasticidin (ThermoFisher Scientific Cat# A1113903) at 48 h post-infection. The expression of *Cas9* was induced by treating cells (48 h) with 2 μg/mL doxycycline (Sigma-Aldrich Cat# D9891) prior to cloning by serial dilution in 96-well plates. Clones were screened by Sanger sequencing (Macrogen) of PCR-amplified genomic fragments of *MAP2K4* (5′-GGTTTGCAGCTCTTGGGATT-3′ and 5′GCCGGTCAGGACCGAGTA-3′) and *MAP2K7* (5′-CCAGCCTAGCTCGGGAAAC-3′and 5′-ATGCTGCGGGGTGTGAAC-3′. The analysis of the genomic DNA sequences was performed using TIDE (50).

Statistical Analysis. All presented data show the mean and SE. GraphPad version 9 was used for statistical analyses. Two-tailed, unpaired *t* test with Welch correction for pairwise comparisons, ANOVA for multiple comparisons, and log-rank tests for Kaplan–Meier analysis and Mann–Whitney *U* test for whole-genome sequencing were performed.

Data, Materials, and Software Availability. Sources for materials used in this study are described in *Materials and Methods* and *SI Appendix*, Table S1. Data are presented Dataset S1 and image data are presented in Dataset S2. Flow cytometry data were deposited in the flow repository database with accession number FR-FCM-Z4UT (52). Genomic DNA sequence data were deposited in the National Center for Biotechnology Information (NCBI) Sequence Read Archive database with accession numbers PRJNA800327 (53) and PRJNA799344 (54), RNA-seq data were deposited in the NCBI Gene Expression Omnibus (GEO) database with accession numbers GSE196459 (55) and GSE200521 (56), and small RNA-seq data were deposited in the NCBI/GEO database with accession number GSE196001 (57). All other study data are included in the article and/or *SI Appendix*.

ACKNOWLEDGMENTS. We thank Kathy Gemme for expert administrative assistance, Dr. Senthil Muthuswamy for providing MCF-10A.B2 cells, and Dr. David Garlick for examining tumor pathology. This study was supported by NIH grants DK107220 and DK112698 (to R.J.D.) and by a Canada Research Chair in Molecular Oncology (Grant # 950-209844 X-216779) and the Canadian Institutes of Health Research (Grants # CIHR FDN-148373 and # CIHR PJT-173401) (to W.J.M.).

Author affiliations: [a]Program in Molecular Medicine, University of Massachusetts Chan Medical School, Worcester, MA 01605; [b]Division of Cancer Sciences, School of Medical Sciences, Faculty of Biology, Medicine and Health, University of Manchester, Manchester M13 9PT, UK; and [c]Department of Biochemistry, Goodman Cancer Research Center, and Faculty of Medicine, McGill University, Montreal, QC H3A 1A3, Canada

1. D. J. Slamon, G. M. Clark, Amplification of c-erbB-2 and aggressive human breast tumors? *Science* **240**, 1795–1798 (1988).
2. J. Staaf *et al.*, Identification of subtypes in human epidermal growth factor receptor 2–positive breast cancer reveals a gene signature prognostic of outcome. *J. Clin. Oncol.* **28**, 1813–1820 (2010).
3. H. Zhong *et al.*, A novel IL6 antibody sensitizes multiple tumor types to chemotherapy including trastuzumab-resistant tumors. *Cancer Res.* **76**, 480–490 (2016).
4. Z. C. Hartman *et al.*, HER2 overexpression elicits a proinflammatory IL-6 autocrine signaling loop that is critical for tumorigenesis. *Cancer Res.* **71**, 4380–4391 (2011).
5. A. Nicolini, A. Carpi, G. Rossi, Cytokines in breast cancer. *Cytokine Growth Factor Rev.* **17**, 325–337 (2006).
6. D. Iliopoulos, H. A. Hirsch, K. Struhl, An epigenetic switch involving NF-κB, Lin28, Let-7 MicroRNA, and IL6 links inflammation to cell transformation. *Cell* **139**, 693–706 (2009).
7. B. Ancrile, K. H. Lim, C. M. Counter, Oncogenic Ras-induced secretion of IL6 is required for tumorigenesis. *Genes. Dev.* **21**, 1714–1719 (2007).
8. M. Rokavec, W. Wu, J. L. Luo, IL6-mediated suppression of miR-200c directs constitutive activation of inflammatory signaling circuit driving transformation and tumorigenesis. *Mol. Cell* **45**, 777–789 (2012).
9. J. S. Han, D. L. Crowe, Jun amino-terminal kinase 1 activation promotes cell survival in ErbB2-positive breast cancer. *Anticancer Res.* **30**, 3407–3412 (2010).
10. R. J. Davis, Signal transduction by the JNK group of MAP kinases. *Cell* **103**, 239–252 (2000).
11. B. L. Bennett *et al.*, SP600125, an anthrapyrazolone inhibitor of Jun N-terminal kinase. *Proc. Natl. Acad. Sci. U.S.A.* **98**, 13681–13686 (2001).
12. J. Bain, H. McLauchlan, M. Elliott, P. Cohen, The specificities of protein kinase inhibitors: An update. *Biochem. J.* **371**, 199–204 (2003).
13. L. A. Garraway, E. S. Lander, Lessons from the cancer genome. *Cell* **153**, 17–37 (2013).
14. C. Tournier *et al.*, Requirement of JNK for stress-induced activation of the cytochrome c-mediated death pathway. *Science* **288**, 870–874 (2000).
15. C. Tournier *et al.*, MKK7 is an essential component of the JNK signal transduction pathway activated by proinflammatory cytokines. *Genes. Dev.* **15**, 1419–1426 (2001).

16. T. Yujiri, S. Sather, G. R. Fanger, G. L. Johnson, Role of MEKK1 in cell survival and activation of JNK and ERK pathways defined by targeted gene disruption. *Science* **282**, 1911–1914 (1998).
17. S. Banerji *et al.*, Sequence analysis of mutations and translocations across breast cancer subtypes. *Nature* **486**, 405–409 (2012).
18. Cancer Genome Atlas, Comprehensive molecular portraits of human breast tumours. *Nature* **490**, 61–70 (2012).
19. G. Ciriello *et al.*, Comprehensive molecular portraits of invasive lobular breast cancer. *Cell* **163**, 506–519 (2015).
20. M. J. Ellis *et al.*, Whole-genome analysis informs breast cancer response to aromatase inhibition. *Nature* **486**, 353–360 (2012).
21. Z. Kan *et al.*, Diverse somatic mutation patterns and pathway alterations in human cancers. *Nature* **466**, 869–873 (2010).
22. S. Nik-Zainal *et al.*, Landscape of somatic mutations in 560 breast cancer whole-genome sequences. *Nature* **534**, 47–54 (2016).
23. S. P. Shah *et al.*, The clonal and mutational evolution spectrum of primary triple-negative breast cancers. *Nature* **486**, 395–399 (2012).
24. P. J. Stephens *et al.*, The landscape of cancer genes and mutational processes in breast cancer. *Nature* **486**, 400–404 (2012).
25. Y. Wang *et al.*, Clonal evolution in breast cancer revealed by single nucleus genome sequencing. *Nature* **512**, 155–160 (2014).
26. A. M. Hudson *et al.*, Truncation- and motif-based pan-cancer analysis reveals tumor-suppressing kinases. *Sci. Signal* **11**, eaan6776 (2018).
27. H. S. Park *et al.*, Akt (protein kinase B) negatively regulates SEK1 by means of protein phosphorylation. *J. Biol. Chem.* **277**, 2573–2578 (2002).
28. S. K. Muthuswamy, D. Li, S. Lelievre, M. J. Bissell, J. S. Brugge, ErbB2, but not ErbB1, reinitiates proliferation and induces luminal repopulation in epithelial acini. *Nat. Cell Biol.* **3**, 785–792 (2001).
29. T. Zhang *et al.*, Discovery of potent and selective covalent inhibitors of JNK. *Chem. Biol.* **19**, 140–154 (2012).
30. M. Das *et al.*, Suppression of p53-dependent senescence by the JNK signal transduction pathway. *Proc. Natl. Acad. Sci. U.S.A.* **104**, 15759–15764 (2007).
31. J. J. Ventura, N. J. Kennedy, R. A. Flavell, R. J. Davis, JNK regulates autocrine expression of TGF-β1. *Mol. Cell* **15**, 269–278 (2004).
32. R. L. Stewart, K. L. O'Connor, Clinical significance of the integrin α6β4 in human malignancies. *Lab. Invest.* **95**, 976–986 (2015).
33. S. J. Lessard *et al.*, JNK regulates muscle remodeling via myostatin/SMAD inhibition. *Nat. Commun.* **9**, 3030 (2018).
34. N. Girnius, Y. J. Edwards, D. S. Garlick, R. J. Davis, The cJUN NH2-terminal kinase (JNK) signaling pathway promotes genome stability and prevents tumor initiation. *Elife* **7**, e36389 (2018).
35. J. Ursini-Siegel *et al.*, ShcA signalling is essential for tumour progression in mouse models of human breast cancer. *EMBO. J.* **27**, 910–920 (2008).
36. J. M. Cejalvo *et al.*, Clinical implications of the non-luminal intrinsic subtypes in hormone receptor-positive breast cancer. *Cancer Treat. Rev.* **67**, 63–70 (2018).
37. F. M. Blows *et al.*, Subtyping of breast cancer by immunohistochemistry to investigate a relationship between subtype and short and long term survival: A collaborative analysis of data for 10,159 cases from 12 studies. *PLoS Med.* **7**, e1000279 (2010).
38. B. Martin-Castillo *et al.*, Basal/HER2 breast carcinomas: Integrating molecular taxonomy with cancer stem cell dynamics to predict primary resistance to trastuzumab (Herceptin). *Cell Cycle* **12**, 225–245 (2013).
39. N. Girnius, R. J. Davis, JNK promotes epithelial cell anoikis by transcriptional and post-translational regulation of BH3-only proteins. *Cell Rep.* **21**, 1910–1921 (2017).
40. C. Cellurale *et al.*, Role of JNK in mammary gland development and breast cancer. *Cancer Res.* **72**, 472–481 (2012).
41. N. Girnius, Y. J. K. Edwards, R. J. Davis, The cJUN NH2-terminal kinase (JNK) pathway contributes to mouse mammary gland remodeling during involution. *Cell Death Differ.* **25**, 1702–1715 (2018).
42. C. C. Davies *et al.*, Impaired JNK signaling cooperates with KrasG12D expression to accelerate pancreatic ductal adenocarcinoma. *Cancer Res.* **74**, 3344–3356 (2014).
43. A. Hubner *et al.*, JNK and PTEN cooperatively control the development of invasive adenocarcinoma of the prostate. *Proc. Natl. Acad. Sci. U.S.A.* **109**, 12046–12051 (2012).
44. M. Van Meter *et al.*, JNK phosphorylates SIRT6 to stimulate DNA double-strand break repair in response to oxidative stress by recruiting PARP1 to DNA breaks. *Cell Rep.* **16**, 2641–2650 (2016).
45. P. C. Calses *et al.*, DGCR8 mediates repair of UV-induced DNA damage independently of RNA processing. *Cell Rep.* **19**, 162–174 (2017).
46. M. Das, D. S. Garlick, D. L. Greiner, R. J. Davis, The role of JNK in the development of hepatocellular carcinoma. *Genes. Dev.* **25**, 634–645 (2011).
47. M. S. Han, T. Barrett, M. A. Brehm, R. J. Davis, Inflammation mediated by JNK in myeloid cells promotes the development of hepatitis and hepatocellular carcinoma. *Cell Rep.* **15**, 19–26 (2016).
48. J. Chen, A. M. Nagle, Y. F. Wang, D. N. Boone, A. V. Lee, Controlled dimerization of insulin-like growth factor-1 and insulin receptors reveals shared and distinct activities of holo and hybrid receptors. *J. Biol. Chem.* **293**, 3700–3709 (2018).
49. F. A. Ran *et al.*, Genome engineering using the CRISPR-Cas9 system. *Nat. Protoc.* **8**, 2281–2308 (2013).
50. E. K. Brinkman, B. van Steensel, Rapid quantitative evaluation of CRISPR genome editing by TIDE and TIDER. *Methods Mol. Biol.* **1961**, 29–44 (2019).
51. L. Naldini *et al.*, In vivo gene delivery and stable transduction of nondividing cells by a lentiviral vector. *Science* **272**, 263–267 (1996).
52. Z. Itah, HER2-driven breast cancer suppression by the JNK signaling pathway. Flow Repository Database. https://flowrepository.org/id/RvFr4uz7ipXXeW7xmMJutwTewVAHsX23IQqsCSyWhBYvfSEAII7HkQpc08TV2s33. Deposited 25 January 2022.
53. Z. Itah, HER2-driven breast cancer suppression by the JNK signaling pathway. NCBI, Sequence Read Archive. https://www.ncbi.nlm.nih.gov/bioproject/PRJNA800327. Deposited 25 January 2022.
54. Z. Itah, HER2-driven breast cancer suppression by the JNK signaling pathway. NCBI, Sequence Read Archive. https://www.ncbi.nlm.nih.gov/bioproject/PRJNA799344. Deposited 21 January 2022.
55. Z. Itah, HER2-driven breast cancer suppression by the JNK signaling pathway. NCBI, GEO. https://www.ncbi.nlm.nih.gov/geo/query/acc.cgi?acc=GSE196459. Deposited 9 April 2022.
56. Z. Itah, HER2-driven breast cancer suppression by the JNK signaling pathway. NCBI, GEO. https://www.ncbi.nlm.nih.gov/geo/query/acc.cgi?acc=GSE200521. Deposited 8 April 2022.
57. Z. Itah, HER2-driven breast cancer suppression by the JNK signaling pathway. NCBI, GEO. https://www.ncbi.nlm.nih.gov/geo/query/acc.cgi?acc=GSE196001. Deposited 2 February 2022.